Available online at www.sciencedirect.com
SCIENCE DIRECT®
Journal of Solid State Chemistry 178 (2005) 1818–1824
JOURNAL OF SOLID STATE CHEMISTRY
www.elsevier.com/locate/jssc

Preparation and characterization of SiO_2/TiO_2 composite microspheres with microporous SiO_2 core/mesoporous TiO_2 shell

Li Zhao, Jiaguo Yu*, Bei Cheng

State Key Laboratory of Advanced Technology for Materials Synthesis and Processing, Wuhan University of Technology, Luoshi road 122#, Wuhan City, Hubei province 430070, PR China

Received 7 January 2005; received in revised form 20 February 2005; accepted 9 March 2005
Available online 7 April 2005

Abstract

SiO_2/TiO_2 composite microspheres with microporous SiO_2 core/mesoporous TiO_2 shell structures were prepared by hydrolysis of titanium tetrabutylorthotitanate (TTBT) in the presence of microporous silica microspheres using hydroxypropyl cellulose (HPC) as a surface esterification agent and porous template, and then dried and calcined at different temperatures. The as-prepared products were characterized with differential thermal analysis and thermogravimetric (DTA/TG), scanning electron microscopy (SEM), X-ray diffraction (XRD), nitrogen adsorption. The results showed that composite particles were about 1.8 μm in diameter, and had a spherical morphology and a narrow size distribution. Uniform mesoporous titania coatings on the surfaces of microporous silica microspheres could be obtained by adjusting the HPC concentration to an optimal concentration of about 3.2 mmol L^{-1}. The anatase and rutile phase in the SiO_2/TiO_2 composite microspheres began to form at 700 and 900 °C, respectively. At 700 °C, the specific surface area and pore volume of the SiO_2/TiO_2 composite microspheres were 552 and 0.652 mL g^{-1}, respectively. However, at 900 °C, the specific surface area and pore volume significantly decreased due to the phase transformation from anatase to rutile.

Keywords: SiO_2/TiO_2 composite microspheres; Microporous core; Mesoporous shell; Phase transformation; High surface area

1. Introduction

Titania has been studied extensively because of its wide application in white pigments for paints, photocatalysts, cosmetics, fillers and photoconductors [1]. The core–shell materials containing titania can improve the properties of the core including chemical, magnetic, and optical properties. Also it can be economical to coat expensive reactants on an inexpensive core [2–5]. However, titania powders with high surface areas are not easily obtained due to phase transformation and crystallite growth. Because of this, efforts to the preparation of SiO_2/TiO_2 composite microspheres have been directed to retard the phase transformation [6,7]. Moreover, SiO_2/TiO_2 composite microspheres may exhibit novel properties that are not found in a single oxide. Recently, it was reported that SiO_2/TiO_2 composite particles exhibited better catalytic properties than the classical oxides such as titania and silica [8]. SiO_2/TiO_2 composite microspheres were good candidate materials for photonic crystals with a complete band gap in the near infrared and visible regions [9,10]. Furthermore, it was found that TiO_2 in SiO_2/TiO_2 composite microspheres exhibited better photoactive than pure TiO_2 particles due to smaller grain size and improved absorption [11–13]. Usually, SiO_2/TiO_2 microspheres could be prepared by many methods including impregnation, precipitation, reverse suspension [14], and sol–gel technology [15–19]. However, the composite microspheres prepared by the above methods showed low surface area due to using non-porous silica as cores. This limited their further potential applications such as catalysis and molecular separations.

*Corresponding author. Fax: +86 27 8788 2395.
E-mail address: jiaguoyu@yahoo.com (J. Yu).

0022-4596/$ - see front matter © 2005 Elsevier Inc. All rights reserved.
doi:10.1016/j.jssc.2005.03.024

Since the invention of MCM 41 [20], many different mesoporous inorganic materials have been synthesized using surfactant-templated method [21]. Recently, Unger et al. [22] reported the synthesis of submicrometer-sized solid core/mesoporous shell (SCMS) silica spheres from the simultaneous sol–gel polymerization of tetraethoxysilane (TEOS) and octadecyltrimethoxysilane (C18TMS) followed by the removal of the organic group. In this paper, it is the first time to report that microporous silica core/mesoporous titania shell composite spheres were synthesized by hydrolysis of titanium tetrabutylorthotitanate (TTBT) in the presence of microporous silica spheres using hydroxypropyl cellulose (HPC) as a surface esterification agent and porous template. The as-prepared products were characterized with differential thermal analysis and thermogravimetric (DTA/TG), scanning electron microscopy (SEM), X-ray diffraction (XRD) and nitrogen adsorption. The microspheres with mesoporous shells show significant advantages over totally porous particles for separating macromolecules [23].

2. Experimental

2.1. Materials

HPC were obtained from Aldrich. Other chemicals used in this study were reagent-grade supplied from Shanghai Chemical Reagent Factory (China). The water used in this work was distilled water.

2.2. Procedures

2.2.1. Preparation of monodispersed microporous silica cores

Monodispersed SiO_2 microporous microspheres were synthesized by a modifying stöber method. In a typical preparation, 1.0 g dodecylamine was dissolved in a mixed solution of ethanol (160 mL) and water (100 mL). Then, 10 mL tetraethoxysilane (TEOS) was added dropwise to the above solution at about 15 °C. The solution was stirred for 4 h, and then the white precipitate was filtrated. The products were repeatedly washed with water and ethanol four times, and then dried at 80 °C for 4 h in a vacuum oven in order to remove water and solvents, and finally calcined at 400 and 600 °C for 4 h in a muffle furnace to remove the templates, respectively. Fig. 1 shows the SEM micrograph of as-prepared silica microspheres. It can be seen that the obtained silica microspheres appear monodispersity and the average diameter of the particles was about more than 600 nm.

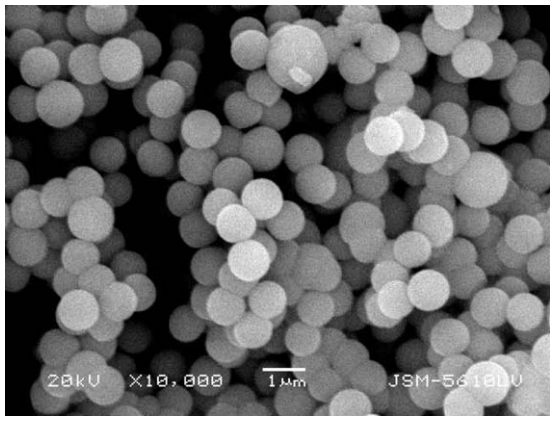

Fig. 1. SEM micrographof monodispersed silica microspheres.

2.2.2. Preparation of the microporous silica core/mesoporous titania shell composite microspheres

1 g microporous silica microspheres obtained by the above method were dispersed in a mixed solution of ethanol (50 mL), water (50 mL) and different concentrations of HPC via sonication. Two milliliter TTBT was dissolved in 20 mL ethanol solution, and then was added into the above mixed solution. The final mixed solution was stirred for 2 h and then the sediment was filtered. The samples were washed twice with ethanol to ensure that the products were completely free from spurious contaminants. The obtained samples were thus dried at 80 °C for 4 h in a vacuum oven in order to remove water and solvents, and finally calcined at 200, 400, 700 and 900 °C for 2 h in a muffle furnace, respectively.

2.3. Characterization

The morphology of the samples was characterized by SEM (type JSM-5610LV) with an accelerating voltage of 20 kV. DTA/TG were performed with a Netzsch STA 449C thermal analyzer in an air flow of 100 mL min^{-1} at a heating rate 10 °C min^{-1} from room temperature to 900 °C. The XRD patterns obtained on an HZG41B-PC X-ray diffractometer using Cu$K\alpha$ radiation at a scan rate $2\theta = 0.05\,^{\circ}s^{-1}$ were used to determine the identity of crystalline phase. The accelerating voltage and applied current were 15 kV and 20 mA, respectively. The Brunauer–Emmett–Teller (BET) surface area (S_{BET}) and pore parameters of the samples were determined with nitrogen adsorption–desorption isotherm measurements at 77 K on a nitrogen adsorption apparatus (Quantachrome ASIC-4). All the samples measured were degassed at 180 °C prior to actual measurements. The BET surface area was determined by the multipoint BET method with the adsorption data in the relative pressure (p/p_0) range 0.1–0.25. The desorption isotherm was used to determine the pore

size distribution using the Horvath–Kawazoe (HK) method [24] and Barret, Joyner, and Halender (BJH) method [25]. The porosity was calculated according to the relation (the skeleton specific volume of SiO_2 is taken as $0.37\,cm^3\,g^{-1}$) [26],

$$P = V_p/(V_p + 0.37), \quad (1)$$

$$V_p = 1.547 \times 10^{-3} V_d, \quad (2)$$

where V_p is the volume of the liquidated nitrogen corresponding to the total pore volume, which was calculated from the saturation adsorption volume at STP, V_d.

3. Results and discussion

3.1. DTA/TG

Fig. 2 shows the DTA/TG curves of SiO_2/TiO_2 composite microsphere sample prepared at a HPC concentration of $3.2\,mmol\,L^{-1}$ and dried at 80 °C for 4 h. The DTA curve shows a broad endothermic peak below 100 °C. This is due to the evaporation of the physically absorbed water and ethanol solvent. Two exothermal peaks at 260 and 345 °C come from the decomposition of organic substances contained in SiO_2/TiO_2 composite microspheres. Furthermore, it can be concluded from our previous research results that the former is assigned to the thermal decomposition of small-molecule organic chemicals in the gels and the latter is due to the combustion of polymer HPC [27,28]. At about 700 °C, a small exothermal peak is observed probably due to the phase transformation of amorphous to anatase. Moreover, the DTA cure also shows a relatively small exothermic peak at about 882 °C. This is caused by the phase transitions from anatase to rutile. The TG curves in Fig. 2 can be divided into three stages. A weight loss (10%) is in the temperature range from room temperature to 100 °C, which can be attributed to the evaporation of the physically adsorbed water and ethanol. The second stage is from 100 to 600 °C. The largest weight loss of about 15% is observed in this stage. This may be the result of the combustion of a large amount of organic residues. In the third stage from 600 to 900 °C, the mass loss is around 2%. This is assigned to the evaporation of chemisorbed water.

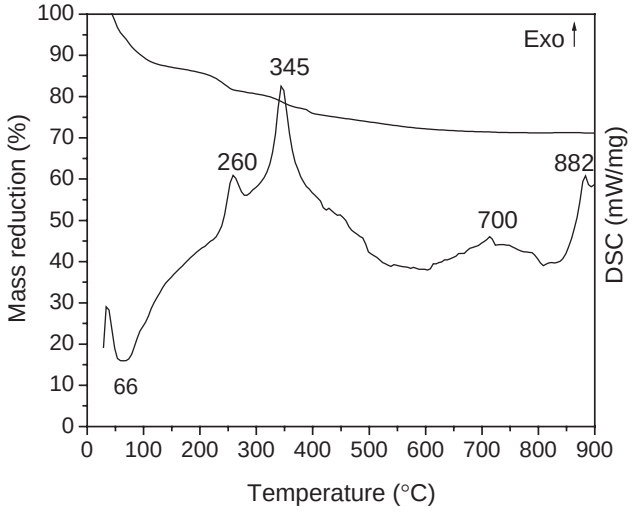

Fig. 2. DTA/TG curves of SiO_2/TiO_2 composite microspheres prepared at a HPC concentration of $3.2\,mmol\,L^{-1}$ and dried at 80 °C for 4 h.

3.2. SEM

Fig. 3 shows the SEM micrographs of the SiO_2/TiO_2 composite microspheres prepared at different HPC concentrations and calcined at 700 °C for 4 h. It can be seen from Fig. 3(a) and (b) that the prepared products appear polydispersity and the coatings are not uniform at [HPC] = 0.32 and $0.96\,mmol\,L^{-1}$. This is probably ascribed to the fact that SiO_2 microspheres are partly coated with TiO_2. At [HPC] = $3.2\,mmol\,L^{-1}$, the average diameter of the SiO_2/TiO_2 composite microspheres obviously becomes large and is about 1.8 μm (Fig. 3(c)). This is probably due to SiO_2 microspheres coated with a thick TiO_2 layer. At [HPC] = $6.4\,mmol\,L^{-1}$, the prepared products appear some small particles among the composite microspheres and the diameter range is from several hundred nanometers to 2 μm (Fig. 3(d)). This is attributed to the fact that, at a higher HPC concentration, the excess HPC caused TiO_2 colloid particles to aggregate and to form TiO_2 aggregated particles. Our experimenal results also showed that if the composite microspheres were prepared in the absence of HPC, SiO_2/TiO_2 composite microspheres could not be obtained.

The formation mechanisms of the SiO_2/TiO_2 composite microspheres may be explained according to the fact that HPC shields the electrostatic repulsive force between SiO_2 and TiO_2 (as shown in Fig. 4). The pH (7.0) of the mixed solution is higher than the isoelectric point of TiO_2 (reported values are 5.6 [29], 5.9 [30] and 6.2 [31]) and SiO_2 (reported values of the isoelectric point of SiO_2 range from 1.8 [32] to 2.7 [33]). Therefore, TiO_2 and SiO_2 colloid particles under these conditions will have a negative surface charge density and will be expected to experience a significant electrostatic repulsion. This means that, at pH 7.0, TiO_2 colloid particles could not deposit on the surface of SiO_2 microspheres due to the electrostatic repulsion between TiO_2 and SiO_2. In order to neutralize the surface charge, a small amount of HPC polymer was added to SiO_2 suspension. A surface esterification reaction between SiO_2 and HPC would occur and these surface charges could be removed

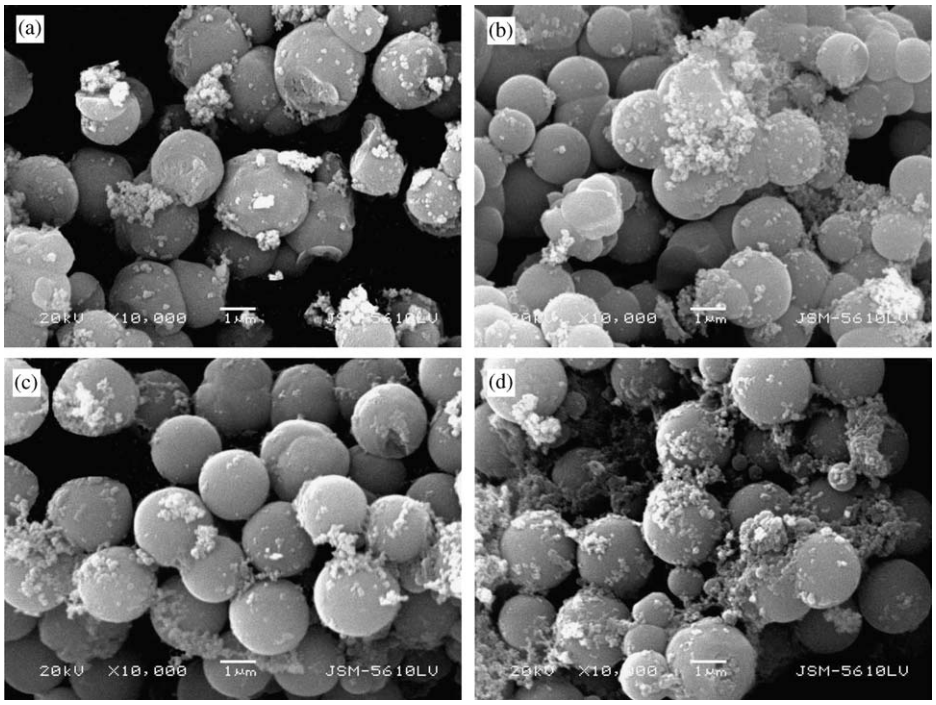

Fig. 3. SEM micrographs of the SiO_2/TiO_2 composite microspheres prepared at [HPC] = 0.32 (a), 0.96 (b), 3.2 (c), and 6.4 (d) mmol L^{-1} and calcined at 700 °C for 2 h, respectively.

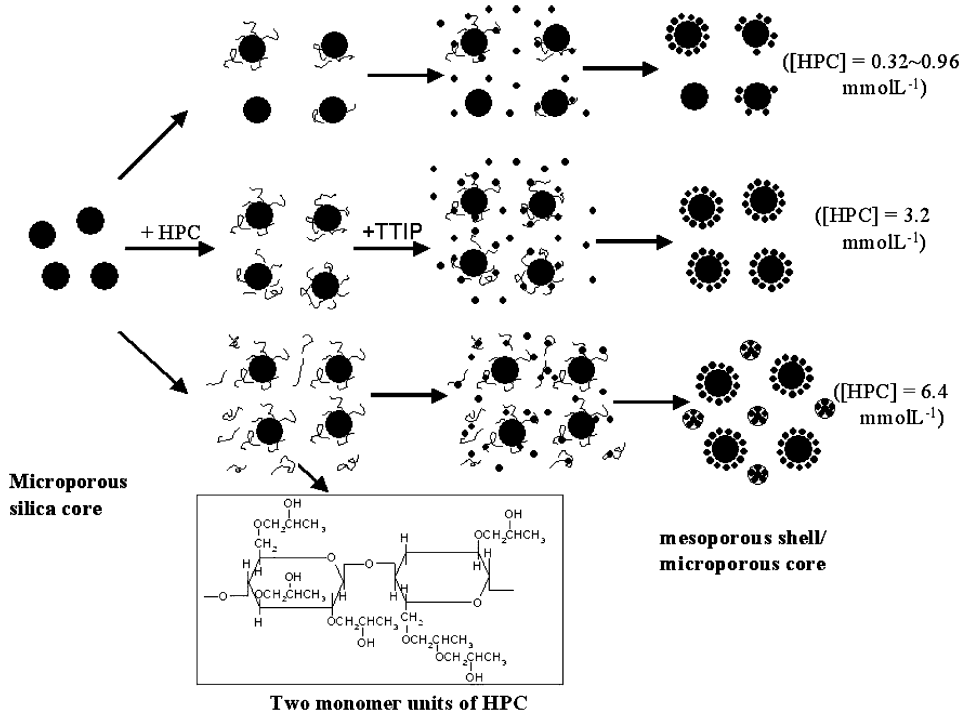

Fig. 4. Schematic model of the formation mechanisms of SiO_2/TiO_2 composite microspheres obtained at different HPC concentrations.

[34–36]. The association between the silica cores and the chains of HPC by hydrogen binding resulted in the enhanced deposition. Since the HPC polymer chains first contacted with the silica cores, then the other segments of the polymer chains also could absorb TiO_2 colloid particles in the solution by hydrogen binding

[37]. As a result, the TiO_2 colloid particles deposited on the surfaces of the silica cores, resulting in the formation of uniform TiO_2 coatings at [HPC] = 3.2 mmol L^{-1}. At a low HPC concentration (from 0.32 to 0.96 mmol L^{-1}), the silica cores were only partly covered by the chains of HPC polymer, which resulted in the formation of non-uniform TiO_2 coatings. On the contrary, at a higher HPC concentration (from 3.2 to 6.4 mmol L^{-1}), a large amount of HPC polymer chains were not only absorbed onto the silica cores but also caused TiO_2 colloid particles to aggregate and to form TiO_2 aggregated particles.

3.3. XRD

Fig. 5 shows the XRD patterns of pure SiO_2 and SiO_2/TiO_2 composite microspheres obtained at a HPC concentration of 3.2 mmol L^{-1} and calcined at different temperatures. At 700 °C, anatase begins to form and its average crystallite size is about 23 nm using Scherrer's equation estimation from anatase (101) plane diffraction peak ($2\theta = 25.4°$). This further confirms that the formation of SiO_2/TiO_2 composite microspheres. Therefore, It can be concluded that the increase of diameter of SiO_2/TiO_2 composite microspheres comes from TiO_2 coating on the surface of SiO_2 microspheres. With increasing calcination temperature, the peak intensity of anatase increases, and the width of the (101) peak becomes narrower. This is due to the growth of anatase crystallites and enhancement of crystallization. At 900 °C, the thermodynamically favored rutile phase begins to appear. The TiO_2 shells contain two phases

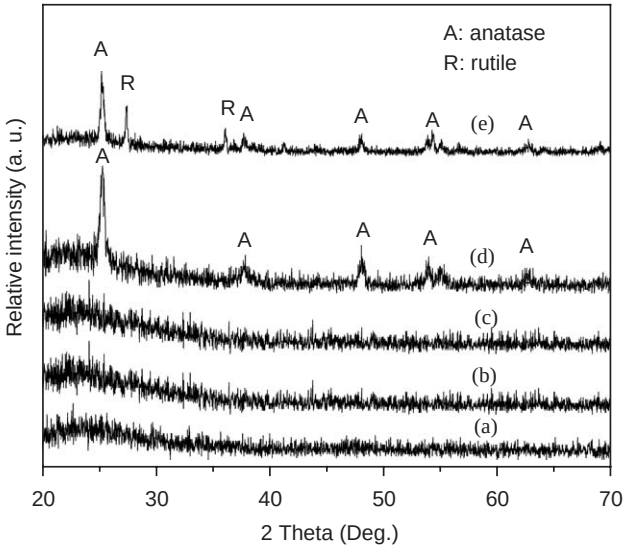

Fig. 5. XRD patterns of pure SiO_2 (a) and SiO_2/TiO_2 composite microspheres (b–e) obtained at a 3.2 mmolL^{-1} HPC concentration and calcined at 200 (b), 400 (c), 700 (d) and 900 °C (e) for 2 h, respectively.

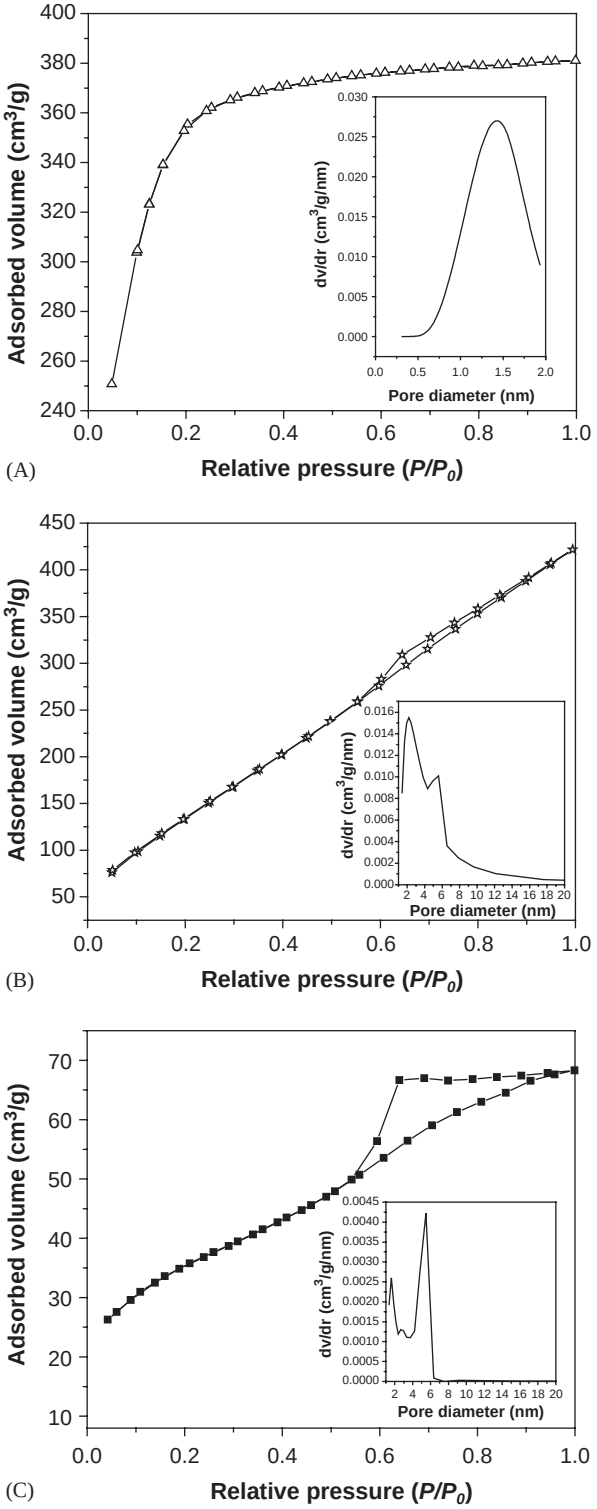

Fig. 6. (A): N_2 adsorption–desorption isotherm of pure SiO_2 microspheres calcined at 600 °C for 4 h and pore size distribution curve of the corresponding products by the HK method; (B and C): N_2 adsorption–desorption isotherm of SiO_2/TiO_2 composite microspheres obtained at a 3.2 mmol L^{-1} HPC concentration and calcined at 700 °C (B) and 900 °C (C) for 2 h, respectively, and pore size distribution curve of the corresponding products by the BJH method.

of anatase and rutile, and their average crystallite sizes are 38 and 66 nm, respectively. From 700 to 900 °C, there is an obvious increase in anatase crystal size due to phase transformation from anatase to rutile as a result of the heat provided to accelerate grain growth [38]. At below 700 °C, there are no diffraction peaks and the TiO_2 shells appear an amorphous state. Usually, for pure TiO_2 samples, the anatase and rutile phases begin to form at 400 and 700 °C, respectively, and the anatase is completely transformed to rutile by about 900 °C. Why is the phase transformation temperature of composite microspheres higher than that of pure titania particles? This is ascribed to the stabilization of the amorphous and anatase TiO_2 phase by the surrounding SiO_2 phase through the TiOSi interface. At the interface, the SiO_2 lattice locks the Ti–O species at the interface of the TiO_2 domains, preventing the nucleation that is necessary for the phase transformation to rutile. Hence, greater heat is required to drive the crystallization [38–42].

3.4. Pore structure characterization

Fig. 6(A) shows the N_2 adsorption–desorption isotherm of pure SiO_2 microspheres and pore size distribution curve of the corresponding products by the HK method. The isotherm of the pure SiO_2 microspheres is a typical Type I isotherm, which indicates that pure SiO_2 microspheres contain a large amount of micropores (as shown in Table 1). Fig. 6(B) and (C) show the N_2 adsorption–desorption isotherm of SiO_2/TiO_2 composite microspheres calcined at 700 °C (B) and 900 °C (C) for 2 h, respectively, and pore size distribution curve of the corresponding products by the BJH method. At 700 °C, the isotherm of SiO_2/TiO_2 composite microspheres (Fig. 6(B)) shows Type I + (IV) isotherm (BDDT classification) [43] with two very distinct regions: at very low relative pressure < 0.4, the isotherm exhibits high adsorption, implies the presence of micropores (type I). However, at high relative pressures between 0.5 and 0.9, the curve exhibits a very small hysteresis loop, indicating the presence of a small amount of mesopores (type IV). The shape of the hysteresis loop is type H2 according to the IUPAC classification [44,45]. This indicated the existence of classic ink-bottle pores. At 900 °C, the isotherm shows a Type (IV) + I. At low relative pressure < 0.4, the isotherm exhibits a relative low adsorption, implies the presence of a small amount of micropores (type I). On the contrary, at high relative pressures between 0.5 and 0.9, the curve exhibits a large hysteresis loop, indicating the presence of a large amount of mesopores (type IV) [45].

Table 1 shows the BET surface areas and pore parameters of pure SiO_2 microspheres and SiO_2/TiO_2 composite microspheres. It can be seen from Table 1 that, at 700 °C, BET surface area and micropore volume of SiO_2/TiO_2 composite microspheres obviously decrease. This is probably due to the increase of TiO_2 amount in the sample. It is also interesting to note that the total pore volume, porosity and HK average pore diameter increase at 700 °C. This is assigned to the existence of mesoporous TiO_2 coating on the surface of SiO_2 microspheres. According to our previous research results, mesopores TiO_2 shells came from the interstitial voids of the packed primary TiO_2 particles on the surface of SiO_2 microspheres [46]. Moreover, HPC can enlarge the mesopores volume as porous template after calcinations. However, at 900 °C, the surface area and total pore volume of the sample significantly decrease. This is attributed to grain growth from the phase transformation of anatase to rutile. Kumar et al. [47] investigated the microstructures of titania membranes calcined at various temperatures by high-resolution scanning electron micrograph. They found that the powders contain small anatase crystallites before the anatase to rutile transformation, but the powders after phase transformation have smaller anatase crystallites and bigger densified rutile regions. It is thought that smaller anatase crystallites grow into bigger rutile crystallites through the transformation, leading to the decrease of the voids among anatase crystallites, which result in the decrease of the surface area and pore volume after calcinations at 900 °C.

Table 1
BET surface areas and pore parameters of SiO_2 microspheres and SiO_2/TiO_2 composite microspheres

Samples	S_{BET}[a] ($m^2 g^{-1}$)	V_p[b] ($mL g^{-1}$)	V_{micro}[c] ($mL g^{-1}$)	Porosity[d] (%)	D[e] (nm)	
					HK	BJH
Pure SiO_2	999	0.4849	0.4121	56.7	1.42	1.62
SiO_2/TiO_2 (700 °C)	552	0.6522	0.4077	63.8	1.56	2.18
SiO_2/ TiO_2 (900 °C)	124	0. 1056	0.0859	22.2	1.50	5.49

[a]BET surface area calculated from the linear part of the BET plot ($P/P_0 = 0.1-0.25$).
[b]Total pore volume, taken from the volume of N_2 adsorbed at $P/P_0 = 0.980$.
[c]Micropore pore volume estimated from the appropriate *t*-plot analysis.
[d]The porosity estimated from the pore volume determined using the adsorption branch of the N_2 isotherm curve at the $P/P_0 = 0.997$ single point.
[e]Average pore diameter estimated using the adsorption branch of the isotherm by the HK and BJH method, respectively.

4. Conclusions

SiO_2/TiO_2 composite microspheres with microporous core/mesoporous shell structures could be prepared by hydrolysis of TTBT in the presence of the microporous silica microspheres using HPC as a surface esterification agent and porous template. The concentration of HPC obviously influences the morphology of SiO_2/TiO_2 composite microspheres. Uniform mesoporous titania coatings could be deposited on the surface of silica microspheres by adjusting the HPC concentration to an optimal HPC concentration at about 3.2 mmol L^{-1}. The composites microspheres contained anatase and rutile phases after calcinations at 900 °C. The composite microspheres overcame the disadvantage of pure TiO_2 powders with low surface areas at high temperature due to the structure of microporous silica core/mesoporous titania shell. This research may provide a new insight into preparation of porous core–shell composite microspheres.

Acknowledgments

This work was supported by the National Natural Science Foundation of China (50272049 and 20473059). This work was also financially supported by the Excellent Young Teachers Program of MOE of China, Project-Sponsored by SRF for ROCS of SEM of China and Key Project of State Key Laboratory of Advanced Technology for Materials Synthesis and Processing (WUT2004Z03).

References

[1] H. Hayashi, K. Torii, J. Mater. Chem. 12 (2002) 3671.
[2] K. Kosuge, P.S. Singh, Chem. Mater. 13 (2001) 2476.
[3] S.D. Shen, B.Z. Tian, C.Z. Yu, S.H. Xie, Z.D. Zhang, B. Tu, D.Y. Zhao, Chem. Mater. 15 (2003) 4046.
[4] C.Z. Yu, Y.H. Yu, D.Y. Zhao, Chem. Commun. 7 (2000) 575.
[5] C.Z. Yu, B.Z. Tian, J. Fan, G.D. Stucky, D.Y. Zhao, J. Am. Chem. Soc. 124 (2002) 4556.
[6] P.K. Nair, F. Mizukami, J. Nair, M. Salou, Y. Oosawa, H. Izutsu, K. Maeda, T. Okubo, Mater. Res. Bull. 33 (1998) 1495.
[7] Y.H. Zhang, A. Reller, Mater. Lett. 57 (2003) 4108.
[8] X.A. Fu, S. Qutubuddin, Colloids Surf. A 178 (2001) 151.
[9] I. Kimura, T. Kase, Y. Taguchi, M. Tanaka, Mater. Res. Bull. 38 (2003) 585.
[10] X.C. Jiang, T. Herricks, Y.N. Xia, Adv. Mater. 15 (2003) 1205.
[11] J.G. Yu, X.J. Zhao, J.C. Yu, G.R. Zhong, J.J. Han, Q.N. Zhao, J. Mater. Sci. Lett. 20 (2001) 1745.
[12] P. Cheng, M.P. Zheng, Y.P. Jin, Q. Huang, M.Y. Gu, Mater. Lett. 57 (2003) 2989.
[13] S.S. Hong, M.S. Lee, S.S. Park, G.D. Lee, Catal. Today 87 (2003) 99.
[14] M. Holgado, A. Cintas, M. Ibisate, C.J. Serna, C. López, F. Meseguer, J. Colloid Interface Sci. 229 (2000) 6.
[15] C.A. Muller, M. Schneider, T. Mallat, A. Baiker, Appl. Catal. A: General 201 (2000) 253.
[16] J. Han, E. Kumacheva, Langmuir 17 (2001) 7912.
[17] K.M.S. Khalil, A.A. Elsamahy, M.S. Elanany, J. Colloid Interface Sci. 249 (2002) 359.
[18] J. Retuert, R. Quijada, V.M. Fuenzalida, J. Mater. Chem. 10 (2000) 2818.
[19] Q.Y. Li, P. Dong, J. Colloid Interface Sci. 261 (2003) 325.
[20] J.C. Vartuli, A. Malek, W.J. Roth, C.T. Kresge, S.B. Mccullen, Micropor. Mesopor. Mater. 44 (2001) 691.
[21] L. Zhao, J.G. Yu, R. Guo, B. Cheng, Key Eng. Mater. 280–283 (2005) 1153.
[22] G. Buchel, K.K. Unger, A. Matsumumoto, K. Tsutsumi, Adv. Mater. 10 (1998) 1036.
[23] J.J. Kirkland, F.A. Truszkowski, C.H. Dilks Jr., G.S. Engel, J. Chromatogr. A 890 (2000) 3.
[24] G. Horvath, K. Kawazoe, J. Chem. Eng Jpn. 16 (1983) 470.
[25] E.P. Barrett, L.G. Joyner, P.H. Halenda, J. Am. Chem. Soc. 73 (1951) 373.
[26] B.D. Yao, L.D. Zhang, J. Mater. Sci. 34 (1999) 5983.
[27] J.G. Yu, X.J. Zhao, Q.N. Zhao, Thin Solid Films 379 (2000) 7.
[28] J.C. Yu, J.G. Yu, L.Z. Zhang, W.K. Ho, J. Photochem. Photobiol. A 148 (2002) 263.
[29] I. Larson, C.J. Drummond, D.Y.C. Chan, F. Grieser, J. Am. Chem. Soc. 115 (1993) 11885.
[30] G.R. Wiese, T.W. Healy, J. Colloid Interface Sci. 51 (1975) 427.
[31] H. Yotsumoto, R.H. Yoon, J. Colloid Interface Sci. 157 (1993) 426.
[32] S. Veeramasuneni, M.R. Yalamanchili, J.D. Miller, Colloids Surf. A 31 (1998) 77.
[33] K. Subramaniam, S. Yiacoumi, C. Tsouris, Colloids Surf. A 177 (2001) 133.
[34] P. Viravathana, D.W.M. Marr, J. Colloid Interface Sci. 221 (2000) 301.
[35] A.K. Van Helden, J.W. Jansen, A. Vrij, J. Colloid Interface Sci. 81 (1981) 354.
[36] A.K. Van Helden, A. Vrij, J. Colloid Interface Sci. 78 (1980) 312.
[37] S.W. Prescott, C.M. Fellows, R.F. Considine, C.J. Drummond, R.G. Gilbert, Polymer 43 (2002) 3191.
[38] J.C. Yu, J.G. Yu, W.K. Ho, Z.T. Jiang, L.Z. Zhang, Chem. Mater. 14 (2002) 3808.
[39] J.C. Yu, J.G. Yu, J.C. Zhao, Appl. Catal. B: Environ. 36 (2002) 31.
[40] C. Anderson, A.J. Bard, J. Phys. Chem. B 101 (1997) 2611.
[41] J.G. Yu, J.C. Yu, M.K.P. Leung, W.K. Ho, B. Cheng, X.J. Zhao, J.C. Zhao, J. Catal. 217 (2003) 69.
[42] J.G. Yu, H.G. Yu, B. Cheng, X.J. Zhao, J.C. Yu, W.K. Ho, J. Phys. Chem. B 107 (2003) 13871.
[43] S. Brunauer, L.S. Deming, W.E. Deming, E. Teller, J. Am. Chem. Soc. 62 (1940) 1723.
[44] K.S.W. Sing, D.H. Everett, R.A.W. Haul, R.A. Pierotti, J. Rouquerol, T. Siemieniewska, Pure Appl. Chem. 57 (1985) 603.
[45] K. Schrijnemakers, E.F. Vansant, J. Porous Mater. 8 (2001) 83.
[46] J.G. Yu, J.C. Yu, W.K. Ho, M.K.P. Leung, B. Cheng, G.K. Zhang, X.J. Zhao, Appl. Catal. A 255 (2003) 309.
[47] K.N.P. Kumar, K. Keizer, A.J. Burggraaf, J. Mater. Chem. 3 (1993) 1141.